International Journal of Technology and Engineering Studies
volume 5 issue 1 pp. 30-36 doi: https://dx.doi.org/10.20469/ijtes.5.10005-1

Finite Element Method Analysis of Densification Process of Sintered Steel for Automobile in Cold Forging

Yuki Morokuma*
Gunma University, Maebashi, Japan

Yuichiro Kamakoshi
Gunma Industrial Technology Center, Maebashi, Japan

Shinichi Nishida
Gunma University, Maebashi, Japan

Ikuo Shohji
Gunma University, Maebashi, Japan

Abstract: The aim of this study is to clarify the effect of the process conditions such as dimensions of material and die, and applied stress on the density distribution in the sintered steel after cold forging by Finite Element Method (FEM) analysis. The analysis model was a porous material model with axial symmetry. A flow stress curve was calculated by a polynomial approximation technique for the true stress-true strain curve obtained by the compression test of the sintered cylindrical specimen. The FEM analysis of cold forging was conducted using a simplified circular cone shape model to increase local density and reduce the cold forging load. In the analysis, a closed die forging model was used. The tip angles of the circular cones and the opening angle of the die were 90, 60 degrees and 120 degrees, respectively. As a result, it was found that the relative density of the tip increases up to 550-600 MPa regardless of the tip angle. Furthermore, the sharper the tip angle, the higher the density enhancement in the tip neighborhood portion.

Keywords: *Powder metallurgy, cold forging, densification, FEM*

Received: 07 December 2018; ***Accepted:*** 11 January 2019; ***Published:*** 24 February 2019

I. INTRODUCTION

Mechanical parts need a stable quality, a reliable supply, a high mass-productivity, and low costs. Furthermore, superior mechanical, chemical, thermal, anti-wear properties are also required for them. Wrought steel has been mainly used for automobile components. Sintered steel has been also adopted in some parts of the components.

However, in recent years, sintered steel has begun to be used in many countries due to demands for further cost reduction [1]. High strength sintered steel has attracted attention. The sintered steel has superior yield rate and enables near-net-shaping, furthermore it has high form accuracy and mass-productivity of complex shape parts (automotive parts such as cams). However, compared with wrought steel, sintered steel is brittle and weak because of inner pores and microstructural defects [2, 3]. These defects are fatal to automotive parts such as cams which are required to have the abrasion resistance and impact resistance.

Many researchers have reported that the mechanical properties of the sintered iron materials such as tensile strength, toughness, fatigue strength, wear resistance, and so on, are improved by the densification [4]. One effective method of achieving a high density of sintered bodies is the sintered cold-forging method [5]. The sintered cold-forging method is a construction method that can greatly improve mechanical properties such as wear resistance and impact resistance by raising density. We focused on the sintered cold-forging method to realize the automobile cam with sintered steel.

In the automobile cam, the mechanical properties

*Correspondence concerning this article should be addressed to Yuki Morokuma, Gunma University, Maebashi, Japan. E-mail: snishida@gunma-u.ac.jp

such as wear resistance and impact resistance are most required to the tip area. Therefore, it is necessary to densify the surface layer of the cam efficiently. We have reported the FEM analysis with density change and plastic deformation by cold-forging using sintered simple specimens [6, 7, 8]. However, there have been few reports on processing conditions to achieve a high density of the tip area in complicated shapes such as the automobile cam by FEM analysis[9, 10]. The aim of this study is to clarify the effect of the process conditions such as dimensions of the forged material and the die, and applied stress on the density distribution in the sintered steel after cold forging by FEM analysis.

II. EXPERIMENTAL PROCEDURE

A. *Specimen and Preparation Method*

In this study, partial diffusion alloyed steel powder (JFE steel, JIP SGM10MO-CMX) for cold-forging was prepared. Tables 1 and 2 show the chemical composition of the iron power and particle size distribution of it, respectively. It is atomized iron powder with diffusional adhered 1 mass% Mo and 0.35 mass% C (graphite powder) to the surface of the powder. Powder compacting was performed using this powder. A metal mold was attached to an electromechanical universal testing machine (TENSHILON TRF-2430), and compacting was performed at a load of 176.5 kN (976.92 MPa to the area of ϕ 15 mm). Three types of punches were prepared: the flat type, the ones to fabricate tip angles of 90 and 60 degrees. Thus, three types of green compacts with a diameter of 15 mm and a height of 15 mm, and a diameter of 15 mm and tip angles of 90 and 60 degrees were prepared.

TABLE 1
CHEMICAL COMPOSITION OF IRON POWDER [MASS%]
(LUBRICANT: 0.5 MASS%)

Element	C	Si	Mn	P	S	Mo	O	Additional Graphite
	0.02	0.01	0.15	0.09	0.006	0.99	0.115	0.35

TABLE 2
PARTICLE SIZE DISTRIBUTION OF IRON POWDER

Particle size (micro meter)	over 180	≥150 <180	≥106 <150	≥75 <106	≥63 <75	≥45 <63	below 45	Total
Ratio[%]	0.1	7.4	18.0	24.7	7.3	20.2	22.3	100

TABLE 3
RELATIVE DENSITY OF OBTAINED SINTERED STEEL

Shape type	Flat	Tip angle: 90 degree	Tip angle: 60 degree
Density [mg/m^3]	7.300	7.276	7.264

The compacts were sintered in a vacuum furnace at a vacuum degree of approximately 30 Pa. The sintering temperature was approximately 1100°C and the sintered time was 60 min. The average density was measured as the apparent density by the Archimedes method. The relative density of the obtained sintered steel is shown in Table 3.

B. *Cold Forging of Sintered Steel*

A punch to fabricate a tip angle of 120 degrees was attached to the top punch of the mold used in the powder compression molding, and cold forging was performed on sintered specimens with tip angles of 90 and 60 degrees. The set load was 176.5 kN which is similar to that in the powder compression molding. The shapes before and after cold forging are shown in Fig. 1.

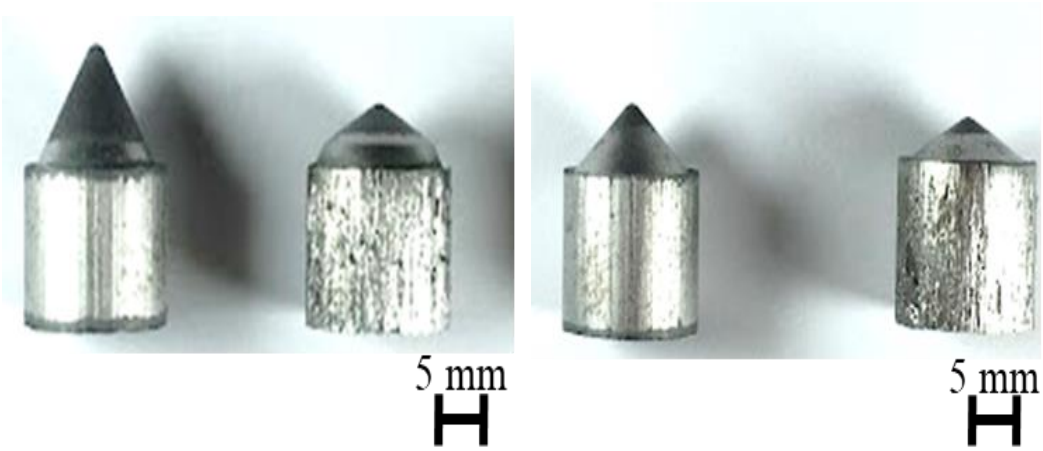

Fig. 1. Shapes before and after cold forging. (a) before forging. Tip angle: 90 degree, (b) after forging. Tip angle: 60 degree.

C. *Compression Test using Sintered Specimen*

To investigate a compression load-stroke (cross head stroke of the testing machine) diagram of sintered materials, the compression test was performed using an electromechanical universal testing machine (TENSILON RTF-2430). To reduce friction force during the test, graphitic lubricant was used and a Teflon sheet was set between the die set and the specimen. The sintered steel with a diameter of 15 mm and a height of 15 mm was used for the compression test. The true stress-true strain diagram was lead from the load-stroke diagram obtained by the compression test. The obtained true stress-true strain diagram was used as material data for the FEM analysis of the porous material.

D. *FEM Analysis*

FEM analysis was performed for the cold forging process of the sintered steel with tip angles of 90 and 60 degrees. For the FEM analysis, DEFORM 2D/3D version 11.0 integrated processing simulation system was used.

III. RESULTS AND DISCUSSION

A. *Determination of Material Data of Sintered Steel*

The true stress-true strain diagram of the sintered steel used for FEM analysis was determined. Firstly, a true stress-true strain diagram was made from a load-stroke diagram obtained by the compression test. FEM analysis was conducted using the true stress-true strain diagram. Fig. 2 shows the 2D analysis model to simulate the compression test. The model was an axisymmetrical one-half model, and both the upper punch and the lower die were a rigid material. The columnar specimen was defined as an elastoplastic material. The conditions of 2D FEM analysis for the compression test are shown in Table 4. The object type of the specimen was defined as rigid-plastic or porous. In order to judge the validity of the experimental value, we analyzed the analytical model as an elastoplastic material and confirmed that the obtained load-stroke diagram agrees with the experimental value. Next, only the analysis model was changed to a porous material, and FEM analysis of the compression test was performed again. The obtained load-stroke diagram showed a lower value than the experimental value. Then, in order to analyze it as a porous material mode, it is necessary to correct the true stress-true strain diagram used for analysis. The corrected true stress-true strain diagram was determined by the method described in the previous paper [6].

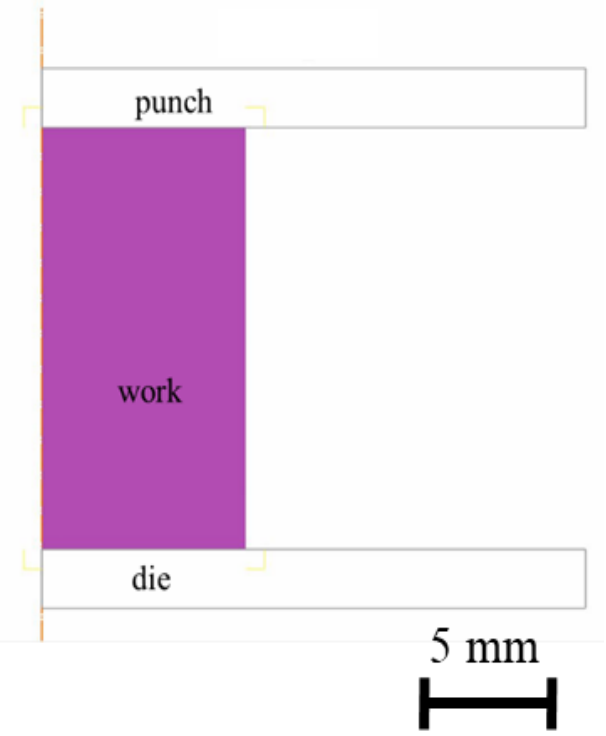

Fig. 2. 2D analysis model for compression test

TABLE 4
CHEMICAL COMPOSITION OF IRON POWDER [MASS%].(LUBRICANT: 0.5 MASS%)

Object Type	Elasto-plastic material	Porous material
Element count [count]	5050	5050
Calculation step [step]	725	725
Step increment [mm/step]	0.01	0.01
Relative density	-	0.945
Shear friction coefficient between a specimen and a punch	0.1	0.1
Shear friction coefficient between a specimen and a punch	0.1	0.1
Remeshing [mm]	0.1	0.1

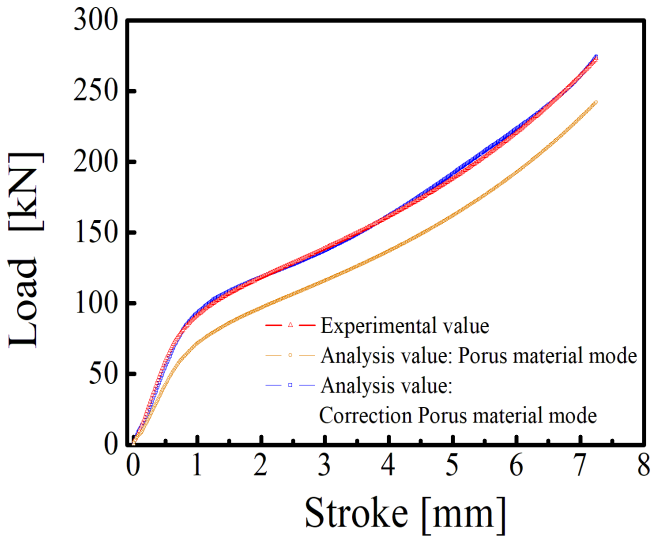

Fig. 3. Load stroke diagram obtained by compression experiment and FEM analysis

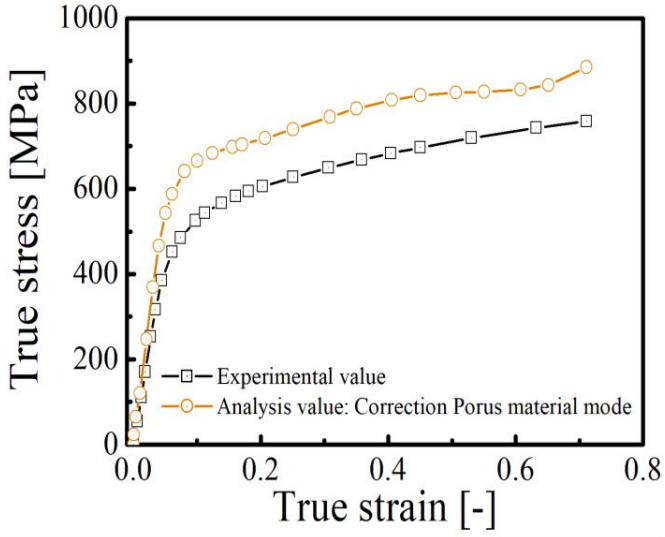

Fig. 4. True stress-true strain diagram obtained from experimental values and a true stress-true strain diagram for corrected porous material mode

Afterward, the FEM analysis of the compression test was performed using the corrected true stress-true strain diagram for the porous material model. As a result, it was confirmed that the obtained load-stroke diagram agreed with the experimental values. Thus the model was adopted as the porous material model. The load-stroke diagrams obtained by experiment values and FEM analysis values are shown in Fig. 3. The true stress-true strain diagram obtained from experimental values and the diagram analyzed by the corrected porous material model are shown in Fig. 4.

B. FEM Analysis of Cold Forging of Sintered Specimen

FEM analysis of cold forging was performed using the corrected true stress-true strain diagram obtained in 3.1. The analysis model is shown in Fig. 5. The model was the axisymmetrical one-half model. To investigate the change in the relative density of the arbitrary positions in the vicinity of the tip, four tracked positions were set in the model as shown in Fig. 5.

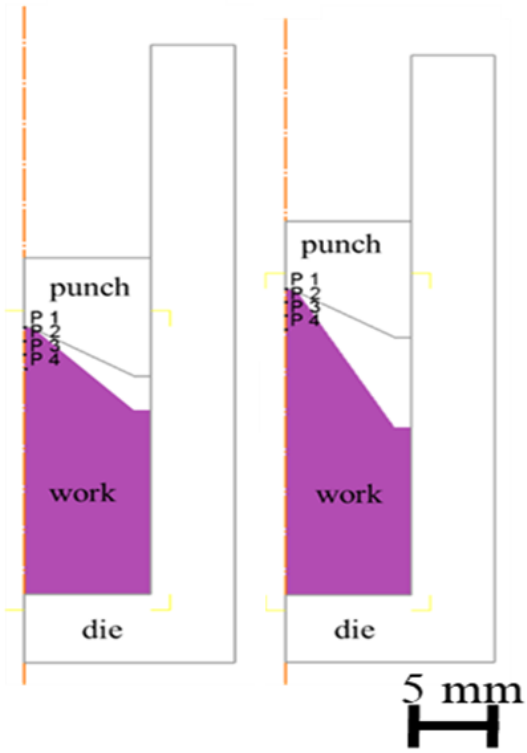

Fig. 5. 2D FEM analysis model for cold forging.
(a) Tip angle: 90 degree (b) Tip angle: 60 degree.

The point P1 was the tip position. The points P2, P3 and P4 were set to the depth direction. The distance from the P1 to P2, P3 and P4 were 1, 2 and 3 mm, respectively. The analysis conditions are shown in Table 5. The initial relative density was 0.945 which is the same value as the columnar specimen. Fig. 6 shows the comparison results of the load stroke diagrams in the cold forging obtained from experimental values and FEM analysis. Although the analytical values showed slightly lower than experimental values at both tip angles, the analytical values almost correspond to the experimental ones.

TABLE 5
CONDITIONS OF 2D FEM ANALYSIS FOR COLD FORGING

Tip angle [degree]	90, 60
Object Type	Porous material
Element count [count]	5050
Calculation step [step]	725
Step increment [mm/step]	0.01
Relative Density	0.945
Shear friction coefficient between a specimen and a punch	0.1
Shear friction coefficient between a specimen and a punch	0.1
Remeshing [mm]	0.1

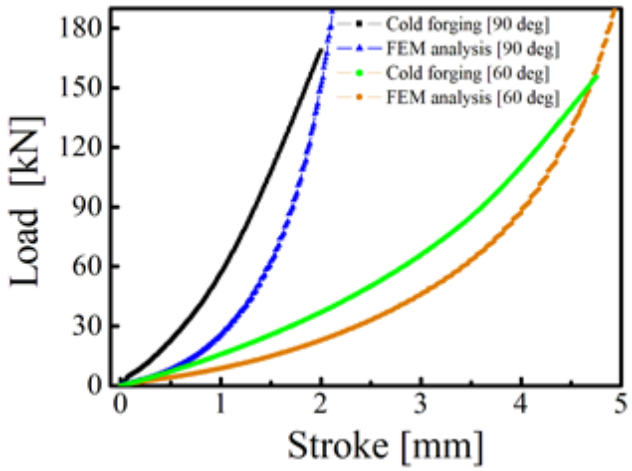

Fig. 6. Comparison results of load stroke diagrams in cold forging obtained from experimental values and FEM analysis

Fig. 7 shows the analysis results of relative density distribution after cold forging. It was found that densification in the tip of the specimen with the tip angle of 60 degrees is promoted compared to that with the tip angle of 90 degrees. It means that large plastic deformation occurs in the tip area of the specimen in the case of the tip angle of 60 degrees.

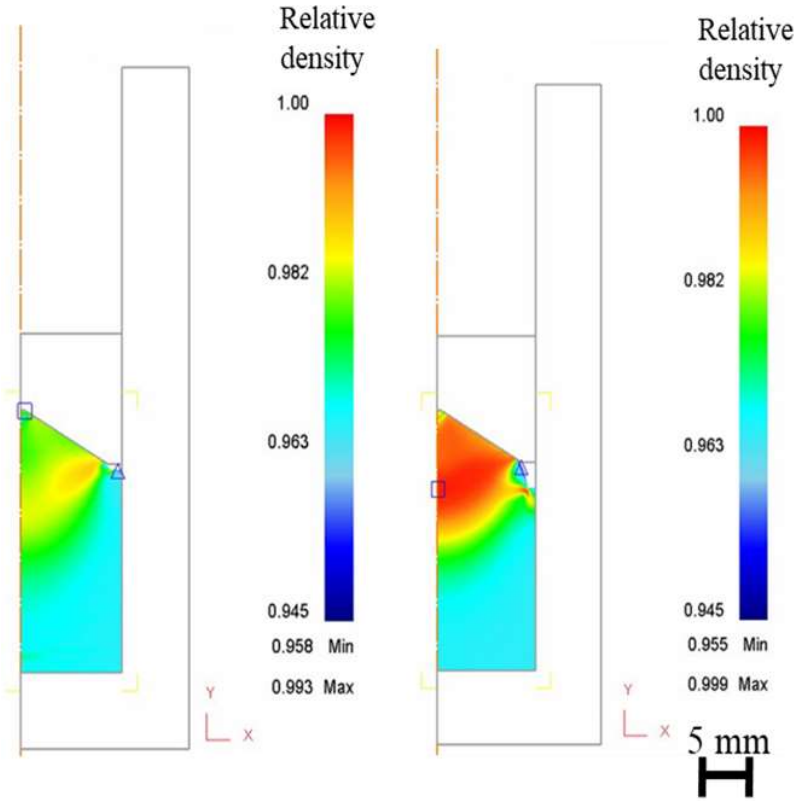

Fig. 7. Analysis results of relative density distribution after cold forging. (a) Tip angle: 90 degree (b) Tip angle: 60 degree

Fig. 8 shows the relationship between the relative density in the tip portion and the load. The relative density abruptly increases within a load of at most 10 kN and saturates to the load of 40 kN regardless of the tip angle and the position. This indicates that the densification is achieved with the plastic deformation of the tip portion at the initial stage of cold forging (up to 40 kN). It was found that the excess applied load hardly affects the densification of the tip portion. The excess applied load could induce a more brittle plastic deformation so that the applied load should be adjusted. Moreover, compared to the densification behavior in the vicinity of the surface layers in the specimens with tip angles of 90 and 60 degrees, it can be seen that densification is promoted in the case of the tip angle of 60 degrees.

Fig. 9 shows the relative density - equivalent stress diagram in both tip angles of 90 and 60 degrees. In the figures, analyzed points at four loads of 40, 80, 100 and 120 kN are also plotted. As described above, the relative density almost saturates more than 40 kN in load. In addition, it was found that equivalent stress also hardly changes more than 40 kN in load. The equivalent stress at the tip position (point P1) was 550-600 MPa regardless of the tip angle. On the other hand, the densification process in the vicinity of the surface layer is realized with higher equivalent stress. After the plastic deformation at the tip position progresses and saturates, the densification process in the vicinity of the tip progresses. Thus, the equivalent stress becomes higher in the tip neighborhood portion.

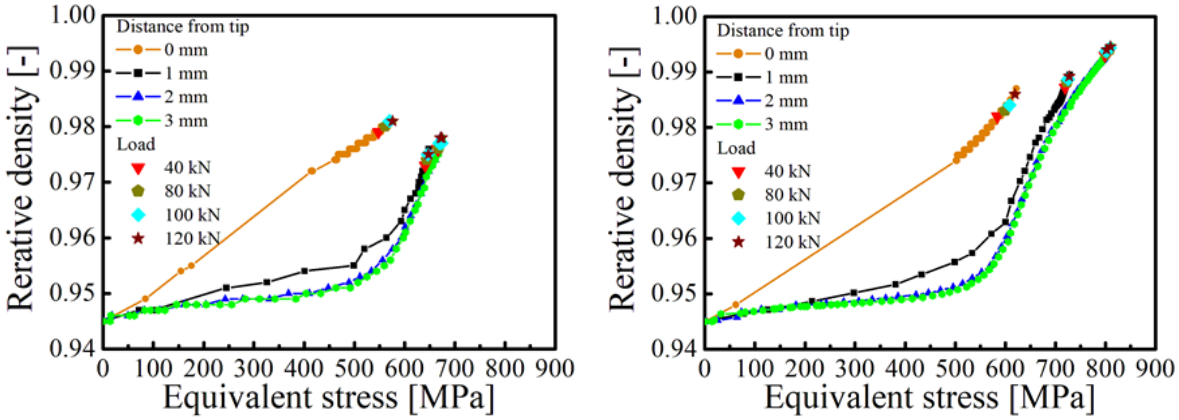

Fig. 8. Relationship between relative density and load. (a) Tip angle: 90 degrees, (b) Tip angle: 60 degrees

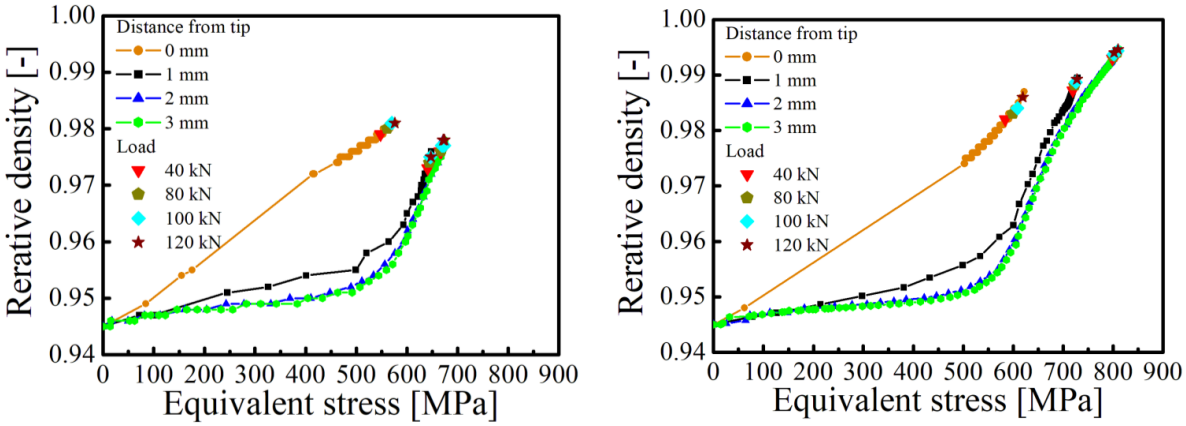

Fig. 9. Relationship between relative density and equivalent stress. (a) Tip angle: 90 degrees, (b) Tip angle: 60 degrees

IV. CONCLUSION

In this study, FEM analysis was conducted for cold forging sintered steel with different tip angles. The effects of the tip angle and load on the densification process near the tip surface layer were investigated. The obtained results are summarized as follows.

1. Plastic deformation and relative density change of conical sintered steel with different tip angles were reproduced by FEM analysis.
2. The relative density abruptly increases within a load of at most 10 kN and saturates to the load of 40 kN regardless of the tip angle and the position investigated.
3. In the case of the load of 40 kN, the equivalent stress in the tip position was 550-600 MPa regardless of the tip angle. On the other hand, since the

densification progresses in the vicinity of the tip even after the plastic deformation at the tip position progresses and saturates, higher equivalent stress is applied in the vicinity of the surface layer.

4. Compared to the tip angle of 90 degrees, the tip angle of 60 degrees is effective to densify the surface layer of the tip in the cold forging.

V. ACKNOWLEDGMENT

This study was operated at Monodukuri Innovation Center, Ota City, Gunma, Japan, and was supported by Monodukuri Research Organization Inc.

REFERENCES

[1] K. S. Narasimhan, "Technology advances for the growth of powder metal in automotive applications," *Japan Society of Powder and Powder Metallurgy*, vol. 54, no. 7, pp. 499–505, 2007. doi: https://doi.org/10.2497/jjspm.54.499

[2] Y. Ozaki, T. Ono, T. Takamiya, and S. Uenosono, "Effects of apparent density on compacting behavior of atomized iron powder," *Journal of the Japan Society of Powder and Powder Metallurgy*, vol. 58, no. 2, pp. 83–90, 2011. doi: https://doi.org/10.2497/jjspm.58.83

[3] L. T. D. Ha and K. M. T. Tsai, "Numerical study on optimization of wooden-steel hybrid beams base on shape factor of steel component," *International Journal of Technology and Engineering Studies*, vol. 1, no. 2, pp. 53–62, 2015. doi: https://doi.org/10.20469/ijtes.40004-2

[4] M. Kondoh, "Development of high accuracy, high density powder compaction technology," *Journal of the Japan Society of Powder and Powder Metallurgy*, vol. 54, no. 7, pp. 506–512, 2007. doi: https://doi.org/10.2497/jjspm.54.506

[5] N. Nakamura, M. Fujinaga, S. Koizumi, and H. Anma, "Sintering and cold-forging process for production of full density sintered materials," *Materia Japan*, vol. 52, no. 2, pp. 80–82, 2013. doi: https://doi.org/10.2320/materia.52.80

[6] Y. Kamakoshi, S. Nishida, K. Kanbe, and I. Shohji, "Finite element method analysis of cold forging for deformation and densification of mo alloyed sintered steel," *IOP Conference Series: Materials Science and Engineering*, vol. 257, pp. 1–11, 2017. doi: https://doi.org/10.1088/1757-899x/257/1/012012

[7] Y. Morokuma, S. Nishida, Y. Kamakoshi, K. Kanbe, T. Kobayashi, and I. Shohji, "Plastic deformation simulation of sintered ferrous material in cold-forging process," *Materials Science Forum*, vol. 941, pp. 552–557, 2018. doi: https://doi.org/10.4028/www.scientific.net/msf.941.552

[8] M. Tufekci, O. E. Genel, and O. Oldac, "Experimental and finite element analysis of vibrations of a rotating annular plates," *Journal of Advances in Technology and Engineering Research*, vol. 3, no. 6, pp. 224–234, 2017. doi: https://doi.org/10.20474/jater-3.6.1

[9] J. D. Wu, Y. C. Luo, and H. Y. Lin, "Experimental and finite element analysis of vibrations of a rotating annular plates," *Journal of Advances in Technology and Engineering Research*, vol. 3, no. 6, pp. 235–243, 2017. doi: https://doi.org/10.20474/jater-3.6.1

[10] H. K. Celik, G. Kunt, A. E. W. Rennie, and I. Akinci, "Non-linear FEM-based shattering simulation of shelled edible agricultural products: Walnut shattering by nut cracker hand tool," *International Journal of Technology and Engineering Studies*, vol. 3, no. 2, pp. 84–92, 2017. doi: https://doi.org/10.20469/ijtes.3.40006-2